

# Supplementary Materials: One-Shot Sequential Federated Learning for Non-IID Data by Enhancing Local Model Diversity

Anonymous Authors

## 1 EXPERIMENTAL SETUP

**Adaptation Details** In an effort to ensure a fair comparison, we adapted the decentralized algorithms DFedAvgM, DFedSAM, and FedSeq to the one-shot setting, and adjusted these methods to select all clients for both training and communication to fit the one-shot setting. This modification means we operate these methods for only one round of communication and select all clients for training and model distribution instead of just a portion, ensuring that all the clients' local data are utilized.

**Implementation Details** In all methods, for local model training, we select the model with the highest validation accuracy as the final model. We employed the Adam optimizer (excluding DFedSAM, which utilized the SAM optimizer) with a learning rate of  $\eta = 5 \times 10^{-5}$  applicable for the CIFAR-10, PACS, and Tiny-ImageNet datasets. Due to the relatively smaller size of the Office-Caltech-10 dataset, we adopted the Adam optimizer with a learning rate of  $\eta = 0.001$ . For the MA-Echo method, we used the learning rate of 0.01 for all datasets as specified in their paper. In all cases, the Adam optimizer's weight decay was fixed at  $1 \times 10^{-4}$ . As for the other hyperparameters of the baselines, we adhered to the values suggested in their papers, which were kept constant and chosen based on optimal validation accuracy. We applied the optimal hyperparameters obtained through the grid-search strategy for our method. Specifically, we set  $E_w$  to 30 for the CIFAR-10 dataset, 20 for all other datasets; we set  $S$  to 5 for the CIFAR-10 dataset, 10 for the PACS and Office-Caltech-10 dataset, and 3 for the Tiny-ImageNet dataset; we set  $\alpha$  to 0.06 for the CIFAR-10 dataset, 1 for the PACS and Tiny-ImageNet dataset, 0.001 for the Office-Caltech-10 dataset; we set  $\beta$  to 1 for the CIFAR-10, PACS and Tiny-ImageNet dataset, 0.001 for the Office-Caltech-10 dataset. During the local training phase of every client, in addition to utilizing scale hyperparameters  $\alpha$  and  $\beta$ , our method also included control over the magnitudes of the distance parameters  $d_1$  and  $d_2$  to one order of magnitude smaller than the original loss  $\ell$ , which was achieved through the logarithmic scaling. For instance, assuming the initial loss  $\ell$  is 6.02 and the original distance  $d_1$  is 45, we would first normalize  $d_1$  to 0.45. Following this, we multiply this normalized distance by the scaling factor  $\alpha$  and subsequently integrate it into the comprehensive loss function  $\mathcal{L}$ . This calibration ensures the original loss maintains primacy in influencing the training process, while the distance regularization terms play an ancillary role, thereby preventing their dominance over the central objective.

**Environment** All our experiments were conducted on a single machine with 1TB RAM and 256-core AMD EPYC 7742 64-Core Processor @ 3.4GHz CPU. The GPU we used is NVIDIA A100 SXM4 with 40GB memory. The software environment settings are: Python 3.7.4, PyTorch 1.13.1 with CUDA 11.6 on Ubuntu 20.04.4 LTS. All the experimental results are the average over three trials.

---

### Algorithm 1: Few-Shot Adaptation of FedELMY

---

**Input:** Local datasets  $\mathcal{D} = \{D_i\}_{i=1}^N$ , warm-up epoch  $E_w$ , learning rate  $\eta$ , number of local iterations  $E_{local}$ , model number to be trained per client  $S$ , scale hyperparameters  $\alpha, \beta$

**Output:** The final model  $m_{final}$

- 1 **Initialization:** For client 1, warm up a randomly initialized model  $m_{avg}^0$  for  $E_w$  epochs
- 2 **for** shot  $r = 1 : T$  **do**
- 3     **for** client  $i = 1 : N$  **do**
- 4         Receives  $m_{avg}^{i-1}$  from client  $i - 1$  (for client 1 from shot  $r > 1$ , receives from client  $N$ )
- 5         // Initialize model pool  $\mathcal{M}^i$  for client  $i$
- 6          $\mathcal{M}^i = \{m_0^i\}$  with  $m_0^i \leftarrow m_{avg}^{i-1}$
- 7         **for**  $j = 1 : S$  **do**
- 8             // Initialize  $m_j^i$
- 9              $m_j^i \leftarrow \frac{1}{|\mathcal{M}^i|} \sum_{t=0}^{|\mathcal{M}^i|-1} m_t^i$
- 10            // Local training for  $m_j^i$
- 11            **for**  $k = 1 : E_{local}$  **do**
- 12                 $\mathcal{L}(m_j^i) \leftarrow \ell(m_j^i; D_i) - \alpha \cdot d_1 + \beta \cdot d_2$
- 13                 $m_j^i \leftarrow m_j^i - \eta \nabla_m \mathcal{L}(m_j^i)$
- 14            **end**
- 15             $\mathcal{M}^i \leftarrow \mathcal{M}^i \cup \{m_j^i\}$
- 16         **end**
- 17          $m_{avg}^i \leftarrow \frac{1}{|\mathcal{M}^i|} \sum_{t=0}^{|\mathcal{M}^i|-1} m_t^i$
- 18         Sends  $m_{avg}^i$  to client  $i + 1$  (for client  $N$ , sends to client 1)
- 19     **end**
- 20 **end**
- 21 // For the final client  $i = N$ , outputs model  $m_{final}$
- 22  $m_{final} \leftarrow m_{avg}^N$

---

## 2 FEW-SHOT ADAPTATION

Alg. 1 illustrates the implementation details and overview of our method in few-shot scenarios. In this scenario, after the local training of the final client  $N$ , it will send its averaged model  $m_{avg}^N$  to the first client 1 to start a new cycle of model training, this process will be repeated for multiple rounds. After completing  $r = T$  iterations, we regard  $m_{avg}^N$  as the final global model  $m_{final}$ .

## 3 ADAPTATION TO DECENTRALIZED PARALLEL FEDERATED LEARNING

Our method can also be adapted to the decentralized Parallel Federated Learning (PFL) setting. Alg. 2 demonstrates the implementation details of our method under the decentralized PFL environment.

**Algorithm 2:** FedELMY for Decentralized PFL

---

**Input:** Local datasets  $\mathcal{D} = \{D_i\}_{i=1}^N$ , warm-up epoch  $E_w$ , learning rate  $\eta$ , number of local iterations  $E_{local}$ , model number to be trained per client  $S$ , scale hyperparameters  $\alpha, \beta$

**Output:** The final model  $m_{final}$

- 1 **Initialization:** For every client  $i$ , warm up a randomly initialized model  $m_0^i$  for  $E_w$  epochs
- 2 **for** client  $i = 1 : N$  **in parallel do**
- 3     // Initialize model pool  $\mathcal{M}^i$  for client  $i$
- 4      $\mathcal{M}^i = \{m_0^i\}$
- 5     **for**  $j = 1 : S$  **do**
- 6         // Initialize  $m_j^i$
- 7          $m_j^i \leftarrow \frac{1}{|\mathcal{M}^i|} \sum_{t=0}^{|\mathcal{M}^i|-1} m_t^i$
- 8         // Local training for  $m_j^i$
- 9         **for**  $k = 1 : E_{local}$  **do**
- 10              $\mathcal{L}(m_j^i) \leftarrow \ell(m_j^i; D_i) - \alpha \cdot d_1 + \beta \cdot d_2$
- 11              $m_j^i \leftarrow m_j^i - \eta \nabla_m \mathcal{L}(m_j^i)$
- 12         **end**
- 13          $\mathcal{M}^i \leftarrow \mathcal{M}^i \cup \{m_j^i\}$
- 14     **end**
- 15      $m_{avg}^i \leftarrow \frac{1}{|\mathcal{M}^i|} \sum_{t=0}^{|\mathcal{M}^i|-1} m_t^i$
- 16     Sends  $m_{avg}^i$  to all other clients  $j = 1 : N, j \neq i$
- 17 **end**
- 18 // For any client  $i = 1 : N$ , output model  $m_{final}$
- 19  $m_{final} \leftarrow \frac{1}{N} \sum_{i=1}^N m_{avg}^i$

---

As we can see, under this setting, clients will train their models concurrently (in parallel). During the training process, each client begins with a randomly initialized model  $m_0^i$ . Upon completion of local training, each client will simultaneously transmit the locally averaged model  $m_{avg}^i$  to all other clients. Once a client  $i$  receives all models from every neighbor, it will calculate an aggregated model by averaging its own averaged model  $m_{avg}^i$  with those received averaged models as the final model  $m_{final}$ . Please note that our framework can also be adjusted for a centralized PFL environment with a central server. In this setup, each client will send its averaged model  $m_{avg}^i$  to the central server. The overall performance will be consistent with that of the decentralized PFL adaptation since the server will finally average all models in a manner identical to the decentralized setting. Experimental results of such an adaptation are shown in Sec. 4.

## 4 ADDITIONAL EXPERIMENTS

In the remaining parts, unless otherwise specified, we set the local training epoch  $E_{local}$  to 200, use the ResNet-18 model structure and follow the Dirichlet distribution  $Dir(0.5)$  for the label-skew tasks in our experiments.

**4.1 Comparison on more datasets.** We compare our method to other baselines on four more public datasets, including both label-skew and domain-shift datasets to enrich our experimental results. As

**Table 1: Test accuracy (%) comparison on more public datasets, including both label-skew and domain-shift datasets.**

Distrubution	Label-Skew		Domain-Shift	
	MNIST	SVHN	Office31	Office-Home
DFedAvgM	11.35±4.01	18.60±5.66	3.47±1.11	1.71±0.23
DFedSAM	12.53±3.93	22.97±4.98	3.49±1.29	1.25±0.32
FedOV	73.10±0.33	37.47±1.48	3.39±0.46	2.31±0.15
DENSE	95.88±1.59	73.76±1.25	3.15±0.58	1.68±0.17
MetaFed	98.07±0.39	76.66±1.78	2.97±0.43	2.40±0.50
FedSeq	98.31±0.65	76.18±2.45	3.46±0.22	2.47±0.29
FedELMY	<b>98.91±0.23</b>	<b>79.55±4.12</b>	<b>3.57±0.09</b>	<b>2.70±0.13</b>

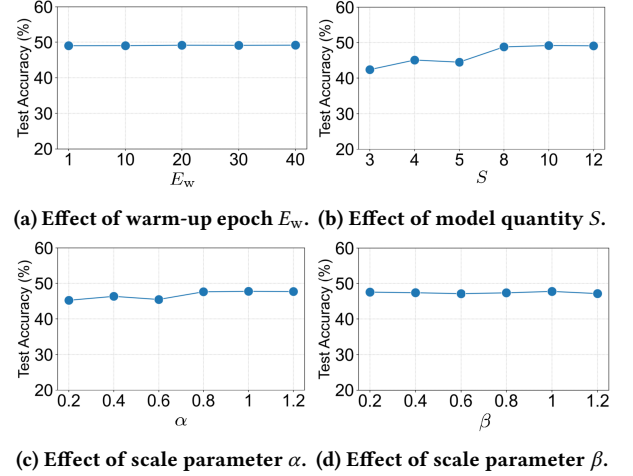


**Figure 1: Grid search results for PACS dataset to investigate the sensitivity of our method to different hyperparameters.**

shown in Table 1, our method consistently outperforms all other baselines on both label-skew and domain-shift scenarios, which further validates the effectiveness of our approach.

**4.2 Hyperparameter sensitivity.** We investigate the sensitivity of our method to different choices of hyperparameters for the PACS dataset as a supplement, as shown in Fig. 1. The findings show that our method maintains consistent robustness irrespective of the search strategies implemented, as observed across all four evaluated hyperparameters (when  $S$  grew to around 10, the performance started to become stable). Such evidence underscores the method's limited reliance on hyperparameter selection.

**4.3 Impact of computation cost.** We show another experiment about the effect of different computation costs on the PACS dataset with Resnet-18 structure. As we can see from Fig. 2, our method can still get the best performance under different computation cost settings, which validates the efficacy of our model training procedures by the diversity-enhanced mechanism.

**4.4 Impact of client numbers.** We assessed the performance of various methods across all datasets by changing the number of clients

**Table 2: Test accuracy (%) comparison of our FedELMY method to other baselines on different numbers of clients  $N$ . For the domain-shift tasks like the PACS dataset, the number of clients  $N = 8$  means we split the whole dataset into 8 parts and allocate them to the clients following the order of “Photo (client 1) → Art-Painting (client 2) → Cartoon (client 3) → Sketch (client 4) → Photo (client 5) → Art-Painting (client 6) → Cartoon (client 7) → Sketch (client 8)” for subsequent training.**

Distribution	Label-Skew								Domain-Shift						
	Dataset	CIFAR-10				Tiny-ImageNet				PACS			Office-Caltech-10		
		5	20	50	100	5	20	50	100	8	20	40	8	20	40
DFedAvgM	21.27	18.22	19.50	24.48	2.64	1.96	1.99	3.09	17.55	16.37	16.62	10.65	9.73	8.94	
DFedSAM	30.62	18.75	10.00	10.01	4.34	2.67	0.64	0.51	16.56	16.48	16.58	14.88	11.58	11.52	
FedOV	41.49	30.93	31.93	38.42	1.33	1.23	1.11	1.08	18.59	17.73	17.32	15.78	10.56	9.34	
DENSE	67.54	52.77	48.38	19.04	3.88	3.03	3.12	3.01	19.18	9.24	14.53	20.72	9.52	11.07	
MetaFed	72.53	57.73	47.47	32.13	31.44	20.46	16.16	13.04	27.33	20.35	16.76	19.43	11.33	11.45	
FedSeq	73.84	64.05	53.62	35.82	31.97	23.38	14.92	15.27	33.01	17.29	12.20	18.40	12.23	9.78	
FedELMY	<b>80.99</b>	<b>68.18</b>	<b>64.31</b>	<b>40.01</b>	<b>38.43</b>	<b>29.52</b>	<b>19.93</b>	<b>20.83</b>	<b>36.10</b>	<b>25.19</b>	<b>23.60</b>	<b>24.45</b>	<b>12.48</b>	<b>12.21</b>	

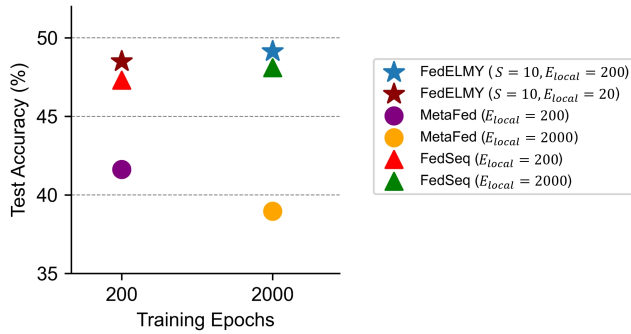


**Figure 2: Test accuracy comparison with different computation costs on PACS dataset.**

**Table 3: Test accuracy (%) comparison of our FedELMY method to other baselines with the CNN model structure.**

Dataset	CIFAR-10	Tiny-ImageNet	PACS	Office-Caltech-10
DFedAvgM	15.08	3.56	20.56	22.84
DFedSAM	13.25	0.49	15.79	9.20
FedOV	53.49	0.69	12.17	22.65
DENSE	61.42	6.72	27.16	34.88
MetaFed	56.11	6.68	28.46	29.99
FedSeq	66.08	14.49	38.36	38.22
FedELMY	<b>69.49</b>	<b>17.05</b>	<b>39.89</b>	<b>39.77</b>

$N$ , as shown in Table 2. It is evident that there is a general trend toward diminishing accuracy for all methods as the client number  $N$  increases, aligning with findings reported in other literature on traditional federated learning. However, it is noteworthy that despite the influence of client quantity on one-shot federated learning, our approach consistently surpasses other baseline methods in performance. To conclude, these experiments consistently confirm the effectiveness and robustness of our proposed method to deal with one-shot sequential federated learning.

**Table 4: Test accuracy (%) comparison of FedELMY to other baselines for different Dirichlet distributions.**

Dataset	CIFAR-10			Tiny-ImageNet		
	$Dir(\cdot)$	0.1	0.3	0.5	0.1	0.3
DFedAvgM	10.33	16.14	18.50	1.07	1.68	2.04
DFedSAM	15.62	21.84	19.48	1.74	2.80	3.41
FedOV	25.92	31.93	45.69	0.94	1.23	1.59
DENSE	26.53	61.73	64.33	1.94	2.37	1.48
MetaFed	27.18	57.24	71.29	9.96	19.45	24.53
FedSeq	27.41	57.91	73.54	15.00	22.23	24.74
FedELMY	<b>29.13</b>	<b>66.32</b>	<b>80.08</b>	<b>16.76</b>	<b>26.85</b>	<b>30.49</b>

**4.5 Impact of model structure.** To evaluate the scalability of our approach, we modified the model structure to a three-layer convolutional neural network (CNN) and replicated the corresponding experiments across all datasets. The results of these tests, which compare the test accuracy of our method to various baseline methods under different scenarios, are presented in Table 3, consistent with the primary analyses reported in the main paper. These findings affirm the robustness and scalability of our proposed method.

**4.6 Impact of data distribution.** To investigate the label-skew scenarios using the CIFAR-10 and Tiny-ImageNet datasets, we performed experiments across varying levels of skew by manipulating the Dirichlet distribution, denoted as  $Dir(\cdot)$ . The results, detailed in Table 4, reveal that our approach outperforms other competing methods in all scenarios, which demonstrates considerable advantages of our method, particularly in terms of scalability and privacy preservation, marking it as a more robust solution in these contexts.

**4.7 PFL Adaptation.** Although our method is not exclusively designed for PFL, we have nevertheless adjusted our algorithm to fit the decentralized PFL setup for a fair comparison. As shown in Table 5, it is evident that our method, even when adapted to the decentralized PFL structure, secures optimal results on most of the datasets relative to other baselines (we compare with MA-Echo [1], which represents the state-of-the-art one-shot decentralized PFL method; DENSE and FedOV which do not conform to the decentralized structure, are excluded from the comparison). It also surpasses

**Table 5: Test accuracy (% , mean±std) comparison of our method under the decentralized PFL setting to other similar baselines with the Resnet-18 model structure.**

Dataset	CIFAR-10	Tiny-ImageNet	PACS	Office-Caltech-10
MA-Echo	10.03±1.38	0.51±0.02	16.70±0.60	11.67±2.39
DFedAvgM	18.59±1.65	2.02±0.20	21.58±2.28	10.01±0.70
DFedSAM	18.51±1.28	3.15±0.29	20.79±1.36	<b>15.09±1.04</b>
FedELMY (PFL)	<b>24.71±2.62</b>	<b>4.12±0.94</b>	<b>24.13±1.57</b>	12.66±1.36

most existing methods on the Office-Caltech-10 dataset. Therefore, our method successfully adapts to various settings and data distributions, highlighting its broad applicability.

## REFERENCES

- [1] Shangchao Su, Bin Li, and Xiangyang Xue. 2023. One-shot Federated Learning without server-side training. *Neural Networks* 164 (2023), 203–215. <https://doi.org/10.1016/j.neunet.2023.04.035>

349  
350  
351  
352  
353  
354  
355  
356  
357  
358  
359  
360  
361  
362  
363  
364  
365  
366  
367  
368  
369  
370  
371  
372  
373  
374  
375  
376  
377  
378  
379  
380  
381  
382  
383  
384  
385  
386  
387  
388  
389  
390  
391  
392  
393  
394  
395  
396  
397  
398  
399  
400  
401  
402  
403  
404  
405  
406

407  
408  
409  
410  
411  
412  
413  
414  
415  
416  
417  
418  
419  
420  
421  
422  
423  
424  
425  
426  
427  
428  
429  
430  
431  
432  
433  
434  
435  
436  
437  
438  
439  
440  
441  
442  
443  
444  
445  
446  
447  
448  
449  
450  
451  
452  
453  
454  
455  
456  
457  
458  
459  
460  
461  
462  
463  
464